HHS Public Access
Author manuscript
Ultrasound Med Biol. Author manuscript; available in PMC 2023 August 01.

Published in final edited form as:
Ultrasound Med Biol. 2022 August ; 48(8): 1663–1671. doi:10.1016/j.ultrasmedbio.2022.04.218.

Added Value of Mass Characteristic Frequency to 2D-Shear Wave Elastography for Differentiation of Benign and Malignant Thyroid Nodules

Jacob Kohlenberg[1,5,#], **Juanjuan Gu**[2,#], **Ahmad Parvinian**[3], **Jeremy Webb**[3], **Omar El Kawkgi**[1], **Nicholas B. Larson**[4], **Mabel Ryder**[1], **Mostafa Fatemi**[2,¶], **Azra Alizad**[3,¶,*]

[1]Department of Medicine, Division of Endocrinology, Mayo Clinic College of Medicine and Science, 200 First Street SW, Rochester, MN 55905, USA

[2]Department of Physiology and Biomedical Engineering, Mayo Clinic College of Medicine and Science, 200 First Street SW, Rochester, MN 55905, USA

[3]Department of Radiology, Mayo Clinic College of Medicine and Science, 200 First Street SW, Rochester, MN 55905, USA

[4]Department of Quantitative Health Sciences, Mayo Clinic College of Medicine and Science, Rochester, MN 55905, USA

[5]Department of Medicine, Division of Diabetes, Endocrinology and Metabolism, University of Minnesota, 420 Delaware St SE, Minneapolis, MN 55455, USA

Abstract

Mass characteristic frequency (f_{mass}) is a novel shear wave (SW) parameter that represents the ratio of the averaged minimum SW speed within the regions of interest to the largest dimension of the mass. Our study objective was to evaluate if the addition of f_{mass} to conventional two-dimensional SW elastography (2D-SWE) parameters would improve the differentiation of benign from malignant thyroid nodules. Our cohort comprised 107 patients with 113 thyroid nodules, of which 67 (59%) were malignant. 2D-SWE data was obtained using the ultrasound system Supersonic Imagine Aixplorer equipped with a 4–15 MHz linear array transducer. A Receiver-Operating Characteristic curve was generated based on a multivariable logistic regression analysis to evaluate the ability of SWE parameters with/without f_{mass} and with/without clinical factors to discriminate benign from malignant thyroid nodules. The addition of f_{mass} to conventional SW elasticity parameters increased the area under the curve from 0.808 to 0.871, p = 0.02. The

[*]**Corresponding author:** Azra Alizad, M.D., Department of Radiology, Mayo Clinic College of Medicine and Science, 200 1st Street SW, Rochester, MN 55905, USA, Phone: (507) 538-1727, Fax: (507) 266-0361, Alizad.Azra@mayo.edu.
[#]Shared first authorship,
[¶]Shared senior authorship

Conflict of Interest Statement
No potential competing interests exist. The authors of this manuscript declare no relationships with any companies, whose products or services may be related to the subject matter of the article. The authors affirm that they do not have any potential financial interest related to the technology referenced in this paper.

combination of SW elasticity parameters plus f_{mass} plus clinical factors provided the strongest thyroid nodule malignancy probability estimate, with a sensitivity of 93.4% and specificity of 91.1% at the optimal threshold. In summary, f_{mass} can be a valuable addition to conventional 2D-SWE parameters.

Keywords

Mass Characteristic Frequency; f_{mass}; Shear Wave Elastography; Thyroid Nodules; Ultrasound

Introduction

Autopsy data suggests that approximately 50% of the general population has at least one thyroid nodule (Bomeli, et al. 2010). Since the vast majority of all thyroid nodules are benign, cost-effective and non-invasive methods of evaluation are essential (Burman and Wartofsky 2016). B-mode ultrasound is the gold standard for non-invasive evaluation of a thyroid nodule. However, ultrasound characteristics of thyroid nodules do not reliably discriminate benign from malignant thyroid nodules, thus, selecting thyroid nodules for fine-needle aspiration (FNA) can be challenging (Chng, et al. 2018).

Therefore, adjunct diagnostic methods have been explored. Increased tissue stiffness is a typical characteristic of malignancy. Because of this, ultrasound elastography, a technique used to assess tissue elasticity, has been introduced as a non-invasive imaging modality to evaluate thyroid nodules (Cosgrove, et al. 2017, Shuzhen 2012, Zhao and Xu 2019). Early elastography techniques, such as strain elastography, required manual external compression and were limited to qualitative evaluation and also relied on operator performance (Ragazzoni, et al. 2012). In two-dimensional shear wave elastography (2D-SWE), ultrasonic focused beams generate acoustic radiation forces that induce shear waves (Bercoff, et al. 2004). Subsequent measurement of the velocity of shear wave propagation allows for the determination of quantitative shear wave elasticity parameters. The SWE technique is less operator dependent and is more quantitative and reproducible than other elastography methods (Chang, et al. 2018). The diagnostic performance of 2D-SWE in differentiating benign from malignant thyroid nodules has varied widely depending on the study, with reported sensitivity ranging from 44% - 95% and specificity ranging from 42% - 94% (Gregory, et al. 2018, Nattabi, et al. 2017).

One limitation of SWE is that elasticity parameters can potentially be affected by multiple factors such as the size and depth of the measured lesion, heterogeneous echogenicity, and the presence of calcifications (Gregory, et al. 2018, Swan, et al. 2019, Yoon, et al. 2013). The anterior wall of the trachea could increase stiffness measurements due to the stress concentration effect, particularly for isthmus nodules, which could be compressed directly against the trachea when the measurement is along the transverse orientation (McQueen and Bhatia 2015). Therefore, the elasticity indices, measured by SWE, may show overlap between malignant and benign nodules, resulting in a lower diagnostic accuracy in the prediction of thyroid malignancy (Swan, et al. 2019). A new shear wave parameter, mass characteristic frequency (f_{mass}), was recently developed to improve the discrimination of benign from malignant lesions (Gu, et al. 2021b). The f_{mass} parameter represents the ratio of the averaged minimum shear wave speed (SWS) within the regions of interest (ROIs) to the largest dimension of the mass. The physical meaning of f_{mass} is the inverse of the maximum shear wave propagation time in a mass (Gu, et al. 2021a). This study is the first to evaluate the performance of f_{mass} in addition to conventional SWE parameters for differentiation of benign from malignant thyroid nodules. The performance of f_{mass} was recently studied in breast cancer, including its correlation with axillary lymph node status, histologic grade, and immunohistochemistry biomarkers and subtypes, as well in predicting the endpoint of neoadjuvant chemotherapy(Gu, et al. 2021a). Our study hypothesizes that the addition of f_{mass} to conventional 2D-SWE parameters can improve the differentiation of benign from malignant thyroid nodules.

Materials and Methods

Study design

In this Institutional Review Board (IRB) approved and Health Insurance Portability and Accountability Act compliant study, subjects who were scheduled for FNA of one or more thyroid nodules were prospectively enrolled. A signed IRB-approved informed written consent with permission for publication was obtained from each volunteer. Subjects were enrolled between March 2015 and March 2020. The decision to obtain an FNA was made by the subject's physician based on ultrasound and clinical parameters, independent of the study team. 108 subjects were recruited and one subject who had Bethesda Category IV cytology without surgical histopathology was excluded (Figure 1) (Cibas, et al. 2009). Ultimately, the study cohort comprised 107 patients with 113 thyroid nodules. The medical record of each subject was reviewed, and demographic information and clinical characteristics were recorded. An experienced radiologist (AP) assessed each subject's B-mode thyroid ultrasound images and classified each nodule using the American College of Radiology (ACR) TI-RADS (Tessler, et al. 2017). Among the 113 thyroid nodules, 79 were TR5 (highly suspicious), 29 were TR4 (moderately suspicious), 4 were TR3 (mildly suspicious), and 1 was TR2 (not suspicious).

The SWE data was obtained prior to FNA. The SWE data was obtained first and subsequently (on the same day) the patient underwent FNA approximately 60 minutes afterward. Thyroid nodule FNA cytology was reported in accordance with the Bethesda System for Reporting Thyroid Cytopathology (Cibas, et al. 2009). Nodules without surgical pathology were classified as benign or malignant based on their respective Bethesda System Category (II, V, VI) and clinical and ultrasound features. For those subjects who underwent lobectomy or thyroidectomy, the histopathologic diagnosis was used.

Shear Wave Elastography Data Acquisition

For each subject, both B-mode and 2D-SWE data were obtained using the commercially available ultrasound system Supersonic Imagine Aixplorer (SSI, Aix-en-Provence, France) that was equipped with a 4–15 MHz linear array transducer. Two expert sonographers operated the transducer for the image acquisition. The SWE measurement was acquired within a rectangle-shaped field of view, which covered the thyroid nodule and the normal adjacent parenchyma. At least six SWE images were obtained for each nodule along each orientation (transverse and longitudinal). The SWE scanning was performed along both the longitudinal and transverse orientations for the majority of subjects. However, some nodules were scanned along the longitudinal orientation only or the transverse orientation only due to subject time constraints. The total nodule number was 113, and this included the nodules that were scanned in both orientations, the longitudinal orientation only, and the transverse orientation only. When thyroid nodules had a heterogeneous composition, SWE was only performed on the solid component, consistent with the World Federation of Ultrasound in Medicine and Biology guidelines (Cosgrove, et al. 2017). To reduce motion artifact, subjects were instructed to halt breathing for three seconds during each acquisition and the sonographers were trained to eliminate hand motion during scanning. The sonographers were instructed to minimize the pressure applied on the probed during scanning (Barr and Zhang 2012, Lam, et al. 2016).

For each orientation, the three SWE images with the least amount of artifact were chosen to draw ROIs. For each SWE image, multiple non-overlapping ROIs, each with a 3 mm diameter, were placed inside the thyroid nodule. Nodules between 5–9 mm had two ROIs and nodules larger than 9 mm had three ROIs. The minimum (E_{min}), maximum (E_{max}), and mean shear wave elasticities (E_{mean}), and the standard deviation of the shear wave elasticity (E_{sd}) for each ROI were calculated automatically by the SSI system, and subsequently averaged over all ROIs for each orientation. The investigative team who performed the measurements was blind to the pathology results.

Mass characteristic frequency was defined as f_{mass} (Hertz (Hz)) = 1000 V_{min}/d, where V_{min} is the minimum SWS (meters/second) and d is the greatest dimension of the thyroid nodule measured from the B-mode images (measured in mm). In this study, f_{mass_long} and f_{mass_trans} are the f_{mass} along the longitudinal and transverse directions, respectively. The relationship between the measured shear wave elasticity and shear wave velocity is $E = 3\rho V^2$, where $\rho = 1000\ kg/m^3$ is medium density, V is the shear wave velocity, and E is the measured shear wave elasticity (Gu, et al. 2021b). Elasticity parameters are defined in Table 1.

Statistical analysis

Quantitative values were summarized by mean ± standard deviation (SD). All statistical analysis was conducted with RStudio (R version 4.0.4, Boston, MA). Testing for distributional differences among the quantitative shear wave parameters by thyroid nodule malignancy status was performed using the Wilcoxon rank-sum test with the pathology results as the gold standard. Two-sided p values less than 0.05 were considered statistically significant. The correlation estimates between shear wave elasticity measurements and thyroid nodule diameter were conducted using the Pearson method. A multivariable logistic regression analysis was performed to assess the association of multiple factors on thyroid nodule pathology and estimate the corresponding probability of malignancy. Receiver operating characteristic (ROC) curve analysis was used to estimate the area under the curve (AUC) and the 95% confidence interval and to determine the cutoff value, as well as the corresponding sensitivity and specificity. Specifically, the optimal cut-point was defined as the point closet to the point (0, 1). Three prediction models were generated in this study using the multivariable logistic regression analysis to discriminate benign from malignant thyroid nodules, and they were the "Trans + Long without f_{mass}" model, the "Trans + Long with f_{mass}" model, and the "Trans + Long with f_{mass} + clinical factors" model. The parameters included in different models were summarized in Table 2. The DeLong test was applied to compare the ROC curves generated with different prediction models. Because of the limited data sample in this study, subjects were not divided into subgroups for prediction model training and validation. Therefore, to address the concern about using the fitted model to evaluate the measures of discrimination performance on the same data set, the AUC adjusted for optimism (Smith, et al. 2014) was also calculated for each prediction model.

Results

There were 107 patients with 113 thyroid nodules included for data analysis (Figure 1a). Subjects' age ranged from 19 to 85 years and the mean (± SD) age was 53.3 ± 16.3 years. Seventy-two (67.3%) of the subjects were women. The thyroid nodule size ranged from 4–65 mm, with a mean (± SD) size of 21.8 ± 13.5 mm. The pathology results were summarized in Figure 1. In total there were 46 benign thyroid nodules and 67 malignant thyroid nodules.

B-mode images and shear wave elastography maps of a malignant and a benign thyroid nodule are depicted in Figures 2 and 3, respectively. For benign thyroid nodules, there was no significant difference in mean or maximum elasticity or f_{mass} based on transducer orientation (Figure 4). However, for malignant thyroid nodules, mean and maximum elasticity and f_{mass} measured significantly greater in the longitudinal plane than the transverse plane (Figure 4). Elasticity parameters were consistently greater for malignant compared to benign thyroid nodules, regardless of the parameter or transducer orientation (Table 3).

The correlation between the thyroid nodule diameter and SWS measured along the transverse orientation was 0.16 (95% CI: 0.02–0.34). The correlation between the thyroid nodule diameter and SWS measured along the longitudinal orientation was −0.07 (95% CI: 0.25–0.11). The presence of thyroid nodule macrocalcifications significantly increased the elasticity parameter f_{mass_long} for malignant but not benign thyroid nodules. Conversely, peripheral rim calcifications had no significant effect on the elasticity parameter f_{mass_long} for either malignant or benign thyroid nodules (Table 4). Thyroid nodules with lobulated or irregular margins had significantly greater E_{mean_long} compared to those with ill-defined margins and those with smooth margins. Avascular thyroid nodules had significantly greater E_{mean_long} compared to vascular nodules. The presence or absence of other ACR TI-RADS and clinical parameters had no significant effect on E_{mean_long}.

A ROC curve analysis was performed to evaluate the ability of different prediction models to discriminate benign from malignant thyroid nodules (Figure 5). The AUC for model "Trans + Long with f_{mass}" was 87.1% (0.80–0.94) and was significantly greater than the model "Trans + Long without f_{mass}" (p=0.02). The AUC for the "Trans + Long with f_{mass} + clinical factors" model was significantly greater than the "Trans + Long with f_{mass}" model (p=0.01). For the model "Trans + Long with f_{mass} + clinical factors", the AUC was 96.9% (95%

CI: 0.94–1.00). The optimism-adjusted AUC for the “Trans + Long without f_{mass}” model, the “Trans + Long with f_{mass}” model and the “Trans + Long with f_{mass} + clinical factors” models was 76.8%, 83.6% and 92.9%, respectively.

Discussion

The objective of this study was to determine whether the addition of f_{mass} to conventional 2D-SWE parameters improved differentiation of benign and malignant thyroid nodules. As expected, we found that elasticity, regardless of ultrasound transducer orientation, was significantly greater in malignant than benign thyroid nodules. This finding is consistent with prior publications and reflects a malignancy-induced increase in tissue stiffness (Cosgrove, et al. 2017, Hu, et al. 2017, Nattabi, et al. 2017). In our study, elasticity was significantly greater in the longitudinal plane compared to the transverse plane for malignant nodules. This likely reflects the anisotropic property of muscle superficial to the thyroid parenchyma (Gennisson, et al. 2010, Gregory, et al. 2018).

We found that the presence of macrocalcifications on B-mode ultrasound imaging increased SWS in malignant thyroid nodules. This was an expected finding and consistent with prior studies, since intranodular calcifications are known to affect lesion stiffness (Chen, et al. 2016, Gregory, et al. 2015, Sun, et al. 2017). Interestingly, we found that peripheral rim calcifications did not significantly affect SWS in either benign or malignant thyroid nodules. Future studies are warranted to investigate the effect of thyroid nodule peripheral rim calcifications on SWS.

In our study, thyroid nodules with lobulated or irregular margins had increased SWS compared to those with ill-defined margins and those with smooth margins. Given that irregular and lobulated thyroid nodule margins are associated with malignancy, this was an expected finding (Tessler, et al. 2017). We found that avascular thyroid nodules had increased SWS compared to vascular nodules. This was unexpected, since thyroid nodule hypervascularity has been associated with malignancy (Baig, et al. 2017). Furthermore, a SWE study on patients with hepatocellular carcinoma (HCC) observed a significantly higher stiffness in hypervascular HCC compared to hypovascular HCC (Ling, et al. 2014). Further studies warranted to correlate the thyroid nodule vascularity with SWE parameters. Other ACR TI-RADS and clinical parameters had no significant effect on shear wave elasticity measurements.

In our study, for SWE data without f_{mass}, the AUC is similar to the results published in multiple meta-analyses that investigated the utility of SWE, with composite sensitivities and specificities ranging from 66%−78% to 78%−87%, respectively (Hu, et al. 2017, Nattabi, et al. 2017, Tian, et al. 2016). We found that the addition of f_{mass} to conventional SWE parameters improved the ability to differentiate benign from malignant thyroid nodules when compared to SWE data without f_{mass}. Moreover, the addition of clinical factors (ACR TI-RADS imaging characteristics and patient gender data) to SWE data with f_{mass} further improved the ability to differentiate benign from malignant thyroid nodules when compared to SWE data with f_{mass}. This improvement was expected because multiple previously published studies demonstrated an increase in AUC when SWE data was analyzed together with TI-RADS imaging characteristics (Pei, et al. 2020, Yang, et al. 2020, Zhang, et al. 2021). However, given the significant differences in patient population, histopathologic diagnoses, TI-RADS classification, and elastography techniques, it is not possible to directly compare the AUC among the studies.

The use of the SWE parameter f_{mass} is novel in the evaluation of thyroid nodules. As expected, the study findings show that f_{mass_long} and f_{mass_trans} are significantly greater in malignant than benign thyroid nodules. We do not propose f_{mass} as a correction for other SWE parameters, but as a new biomarker for lesion characterization. The impetus for calculating f_{mass} was to reduce the probability of a type II error given that with SWE, the SWS of smaller masses can be underestimated (Gu, et al. 2020, Gu, et al. 2022). In malignant breast lesions it has been shown that SWS can be significantly underestimated with tumors less than 10 mm (Yoon, et al. 2013). Because f_{mass} signifies SWS relative to the inverse of mass diameter, f_{mass} assumes a larger value for smaller masses. The findings in our study support the use of f_{mass} in the evaluation of thyroid nodules since the addition of f_{mass} to the other SWE parameters significantly improved the differentiation of benign from malignant thyroid nodules.

In this study, weak correlations were found between thyroid nodule diameter and SWS measured along the longitudinal and transverse orientations. This implies that the correlation between minimum SWS and thyroid nodule diameter will not directly affect the performance of f_{mass}. This result is consistent with the findings in a recent publication (Gu, et al. 2021b).

One potential limitation with f_{mass} is the method used to measure thyroid nodule diameter. In this study, f_{mass} was calculated using the largest thyroid nodule diameter visualized on a B-mode ultrasound image. A potential source of error is the measurement of diameter in a nodule with an irregular, lobulated, or poorly defined margin. In such cases, alternative methods to assess diameter can be using an ellipse to approximate nodule morphology or measure the perimeter of the nodule and calculate the equivalent circular diameter (Gu, et al. 2021b). Future studies can refine the calculation of f_{mass} by evaluating the optimal approach to determining lesion diameter. A limitation to the study was the relatively smaller number of thyroid nodules with Bethesda category III or IV cytology with surgical histopathology. This prevented a subgroup analysis of these subjects to determine if f_{mass} is useful in the evaluation of thyroid nodules with indeterminate cytology. Another limitation is that it is challenging to measure the minimum shear wave velocity in masses with sold and cystic areas (Hindi, et al. 2013).

Conclusions

In conclusion, the study findings show the new SWE parameter, mass characteristic frequency (f_{mass}), which is novel in the evaluation of thyroid nodules, can be a valuable addition to conventional 2D-SWE parameters and improves the differentiation of benign from malignant thyroid nodules. Combining conventional SWE parameters with f_{mass} and clinical factors (ACR TI-RADS imaging characteristics and patient gender) increases the strength of the malignancy probability estimate of a thyroid nodule. Future studies should prospectively evaluate a risk prediction score that incorporates SWE data including f_{mass} together with TI-RADS and clinical characteristics to aid the clinician in the selection of thyroid nodules for FNA.

Acknowledgments

The authors would like to thank Dr. Max Denis, PhD; Dr. Mahdi Bayat, PhD; Dr. Viksit Kumar, PhD; Dr. Bae-Hyung Kim, PhD; Dr. Rohit Nayak, PhD; Dr. Saba Adabi, PhD; Dr. Redouane Ternifi, PhD; Ms. Adriana Gregory, MS; and Ms. Yinong Wang, MS, for their assistance in SWE data acquisition at different time periods during the course of the study. Also, we thank Mr. Duane Meixner, R.V.T., R.D.M.S., and Ms. Kate Knoll, R.V.T., R.D.M.S for patient scanning and Ms. Theresa Nelson, Barbara Foreman and Ms. Cindy Andrist for their valuable help in patient recruitment.

The study was supported by the grants from the National Institutes of Health 1R01EB017213 from National Institute of Biomedical Imaging and Bioengineering and R01CA195527 and R01CA168575. R01CA148994 from National Cancer Institute as well as a grant from National Science Foundation CNS-1837572. The content is solely the responsibility of the authors and does not necessarily represent the official views of the NIH. The NIH did not have any additional role in the study design, data collection and analysis, decision to publish or preparation of the manuscript.

References

Baig FN, Lunenburg JTJV, Liu SYW, Yip SP, Law HKW, Ying M. Computer-aided assessment of regional vascularity of thyroid nodules for prediction of malignancy. Sci Rep 2017; 7:14350. [PubMed: 29084994]

Baig FN, Lunenburg JTJV, Liu SYW, Yip SP, Law HKW, Ying M. Computer-aided assessment of regional vascularity of thyroid nodules for prediction of malignancy. Sci Rep 2017; 7:14350. [PubMed: 29084994]

Barr RG, Zhang Z. Effects of precompression on elasticity imaging of the breast: development of a clinically useful semiquantitative method of precompression assessment. J Ultrasound Med 2012; 31:895–902. [PubMed: 22644686]

Bercoff J, Tanter M, Fink M. Supersonic shear imaging: a new technique for soft tissue elasticity mapping. IEEE Trans Ultrason Ferroelectr Freq Control 2004; 51:396–409. [PubMed: 15139541]

Bomeli SR, LeBeau SO, Ferris RL. Evaluation of a thyroid nodule. Otolaryngol Clin North Am 2010; 43:229–38, vii. [PubMed: 20510711]

Burman KD, Wartofsky L. Thyroid Nodules. N Engl J Med 2016; 374:1294–5.

Chang N, Zhang X, Wan W, Zhang C. The Preciseness in Diagnosing Thyroid Malignant Nodules Using Shear-Wave Elastography. Med Sci Monit 2018; 24:671–77. [PubMed: 29391387]

Chen BD, Xu HX, Zhang YF, Liu BJ, Guo LH, Li DD, Zhao CK, Li XL, Wang D, Zhao SS. Calcification of thyroid nodules increases shear-wave speed (SWS) measurement: using multiple calcification-specific SWS cutoff values outperforms a single uniform cutoff value in diagnosing malignant thyroid nodules. Oncotarget 2016; 7:66149–59. [PubMed: 27588492]

Chng CL, Tan HC, Too CW, Lim WY, Chiam PPS, Zhu L, Nadkarni NV, Lim AYY. Diagnostic performance of ATA, BTA and TIRADS sonographic patterns in the prediction of malignancy in histologically proven thyroid nodules. Singapore Med J 2018; 59:578–83. [PubMed: 29774361]

Cibas ES, Ali SZ, Conference NCITFSotS. The Bethesda System For Reporting Thyroid Cytopathology. Am J Clin Pathol 2009; 132:658–65. [PubMed: 19846805]

Cosgrove D, Barr R, Bojunga J, Cantisani V, Chammas MC, Dighe M, Vinayak S, Xu JM, Dietrich CF. WFUMB Guidelines and Recommendations on the Clinical Use of Ultrasound Elastography: Part 4. Thyroid. Ultrasound Med Biol 2017; 43:4–26. [PubMed: 27570210]

Gennisson JL, Deffieux T, Macé E, Montaldo G, Fink M, Tanter M. Viscoelastic and anisotropic mechanical properties of in vivo muscle tissue assessed by supersonic shear imaging. Ultrasound Med Biol 2010; 36:789–801. [PubMed: 20420970]

Gregory A, Bayat M, Kumar V, Denis M, Kim BH, Webb J, Meixner DD, Ryder M, Knudsen JM, Chen S, Fatemi M, Alizad A. Differentiation of Benign and Malignant Thyroid Nodules by Using

Combpush Ultrasound Shear Elastography: A Preliminary Two-plane View Study. Acad Radiol 2018; 25:1388–97. [PubMed: 29573939]

Gregory A, Mehrmohammadi M, Denis M, Bayat M, Stan DL, Fatemi M, Alizad A. Effect of Calcifications on Breast Ultrasound Shear Wave Elastography: An Investigational Study. PLoS One 2015; 10:e0137898. [PubMed: 26368939]

Gu J, Polley EC, Boughey JC, Fazzio RT, Fatemi M, Alizad A. Prediction of Invasive Breast Cancer Using Mass Characteristic Frequency and Elasticity in Correlation with Prognostic Histologic Features and Immunohistochemical Biomarkers. Ul Trasound Med Biol 2021b.

Gu J, Polley EC, Denis M, Carter JM, Pruthi S, Gregory AV, Boughey JC, Fazzio RT, Fatemi M, Alizad A. Early assessment of shear wave elastography parameters foresees the response to neoadjuvant chemotherapy in patients with invasive breast cancer. Breast Cancer Res 2021a; 23:1–13. [PubMed: 33407744]

Gu J, Polley EC, Ternifi R, Nayak R, Boughey JC, Fazzio RT, Fatemi M, Alizad A. Individualized-thresholding Shear Wave Elastography combined with clinical factors improves specificity in discriminating breast masses. Breast 2020; 54:248–55. [PubMed: 33188991]

Gu J, Ternifi R, Larson NB, Carter JM, Boughey JC, Stan DL, Fazzio RT, Fatemi M, Alizad A. Hybrid highdefinition microvessel imaging/shear wave elastography improves breast lesion characterization. Breast Cancer Research 2022; 24:1–13. [PubMed: 34983617]

Hindi A, Peterson C, Barr RG. Artifacts in diagnostic ultrasound. Reports in Medical Imaging 2013; 6:29–48.

Hu X, Liu Y, Qian L. Diagnostic potential of real-time elastography (RTE) and shear wave elastography (SWE) to differentiate benign and malignant thyroid nodules: A systematic review and meta-analysis. Medicine (Baltimore) 2017; 96:e8282. [PubMed: 29068996]

Lam AC, Pang SW, Ahuja AT, Bhatia KS. The influence of precompression on elasticity of thyroid nodules estimated by ultrasound shear wave elastography. Eur Radiol 2016; 26:2845–52. [PubMed: 26607575]

Ling W, Lu Q, Lu C, Quan J, Ma L, Li J, He D, Liu J, Yang J, Wen T. Effects of vascularity and differentiation of hepatocellular carcinoma on tumor and liver stiffness: in vivo and in vitro studies. Ul Trasound Med Biol 2014; 40:739–46.

McQueen AS, Bhatia KS. Thyroid nodule ultrasound: technical advances and future horizons. Insights into imaging 2015; 6:173–88. [PubMed: 25736837]

Nattabi HA, Sharif NM, Yahya N, Ahmad R, Mohamad M, Zaki FM, Yusoff AN. Is Diagnostic Performance of Quantitative 2D-Shear Wave Elastography Optimal for Clinical Classification of Benign and Malignant Thyroid Nodules?: A Systematic Review and Meta-analysis. Acad Radiol 2017.

Pei S, Zhang B, Cong S, Liu J, Wu S, Dong Y, Zhang L, Zhang S. Ultrasound Real-Time Tissue Elastography Improves the Diagnostic Performance of the ACR Thyroid Imaging Reporting and Data System in Differentiating Malignant from Benign Thyroid Nodules: A Summary of 1525 Thyroid Nodules. Int J Endocrinol 2020; 2020:1749351. [PubMed: 32351557]

Ragazzoni F, Deandrea M, Mormile A, Ramunni MJ, Garino F, Magliona G, Motta M, Torchio B, Garberoglio R, Limone P. High diagnostic accuracy and interobserver reliability of real-time elastography in the evaluation of thyroid nodules. Ul Trasound Med Biol 2012; 38:1154–62.

Shuzhen C Comparison analysis between conventional ultrasonography and ultrasound elastography of thyroid nodules. Eur J Radiol 2012; 81:1806–11. [PubMed: 21962937]

Smith GC, Seaman SR, Wood AM, Royston P, White IR. Correcting for optimistic prediction in small data sets. American journal of epidemiology 2014; 180:318–24. [PubMed: 24966219]

Sun CY, Lei KR, Liu BJ, Bo XW, Li XL, He YP, Wang D, Ren WW, Zhao CK, Xu HX. Virtual touch tissue imaging and quantification (VTIQ) in the evaluation of thyroid nodules: the associated factors leading to misdiagnosis. Sci Rep 2017; 7:41958. [PubMed: 28157195]

Swan KZ, Bonnema SJ, Jespersen ML, Nielsen VE. Reappraisal of shear wave elastography as a diagnostic tool for identifying thyroid carcinoma. Endocrine connections 2019; 8:1195–205. [PubMed: 31340198]

Swan KZ, Bonnema SJ, Jespersen ML, Nielsen VE. Reappraisal of shear wave elastography as a diagnostic tool for identifying thyroid carcinoma. Endocr Connect 2019; 8:1195–205. [PubMed: 31340198]

Tessler FN, Middleton WD, Grant EG, Hoang JK, Berland LL, Teefey SA, Cronan JJ, Beland MD, Desser TS, Frates MC, Hammers LW, Hamper UM, Langer JE, Reading CC, Scoutt LM, Stavros AT. ACR Thyroid Imaging, Reporting and Data System (TI-RADS): White Paper of the ACR TI-RADS Committee. J Am Coll Radiol 2017; 14:587–95. [PubMed: 28372962]

Tian W, Hao S, Gao B, Jiang Y, Zhang X, Zhang S, Guo L, Yan J, Luo D. Comparing the Diagnostic Accuracy of RTE and SWE in Differentiating Malignant Thyroid Nodules from Benign Ones: a Meta-Analysis. Cell Physiol Biochem 2016; 39:2451–63. [PubMed: 27832644]

Yang JR, Song Y, Xue SS, Ruan LT. Suggested amendment of TI-RADS classification of thyroid nodules by shear wave elastography. Acta Radiol 2020; 61:1026–33. [PubMed: 31825762]

Yoon JH, Jung HK, Lee JT, Ko KH. Shear-wave elastography in the diagnosis of solid breast masses: what leads to false-negative or false-positive results? Eur Radiol 2013; 23:2432–40. [PubMed: 23673572]

Zhang WB, Xu W, Fu WJ, He BL, Liu H, Deng WF. Comparison of ACR TI-RADS, Kwak TI-RADS, ATA guidelines and KTA/KSThR guidelines in combination with SWE in the diagnosis of thyroid nodules. Clin Hemorheol Microcirc 2021; 78:163–74. [PubMed: 33579829]

Zhao CK, Xu HX. Ultrasound elastography of the thyroid: principles and current status. Ultrasonography 2019; 38:106–24. [PubMed: 30690960]

Author Manuscript

Author Manuscript

Author Manuscript

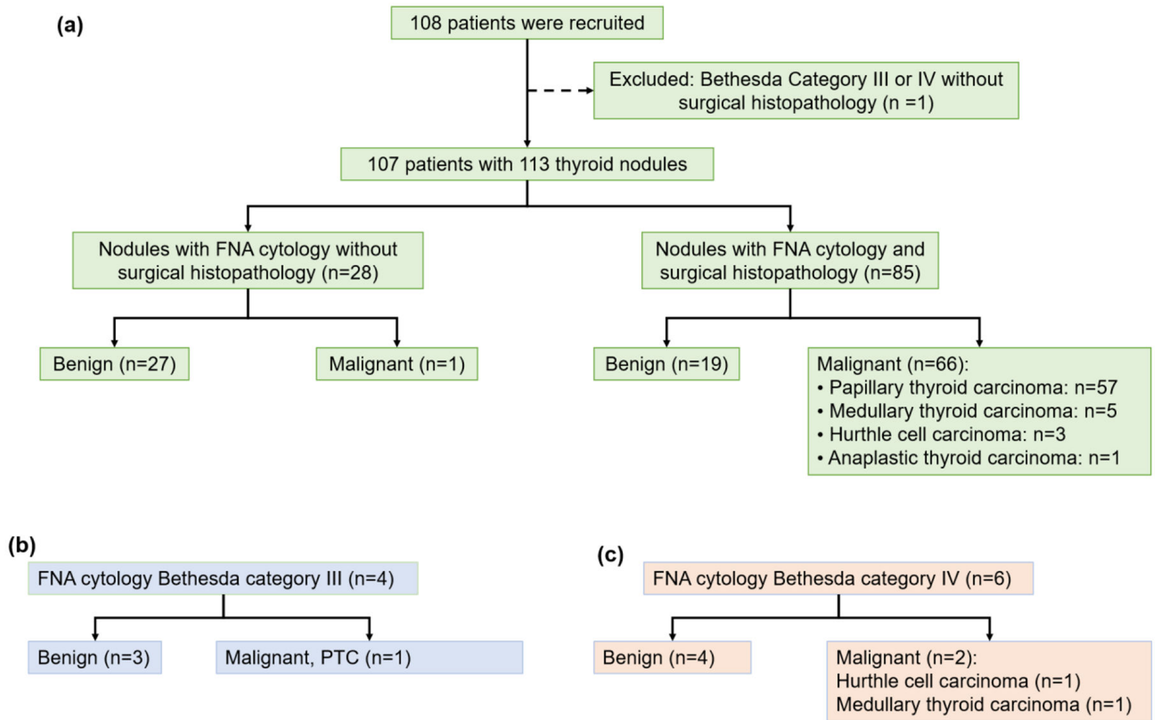

Figure 1: Surgical histopathology and cytology.

(**a**) Of the 108 patients recruited to the study, one with Bethesda Category IV cytology without surgical histopathology was excluded prior to data analysis. The remaining 107 patients with 113 thyroid nodules all had shear wave elastography data obtained using the ultrasound system Supersonic Imagine Aixplorer (SSI, Aix-en-Provence, France) that was equipped with a 4–15 MHz linear array transducer. Of the 28 nodules without surgical histopathology, 27 were benign based on Bethesda Category II cytology and/or clinical follow-up and one patient had a malignant nodule (Bethesda Category VI). There were 10 nodules with indeterminate FNA cytology, (**b**) 4 Bethesda Category III cytology (Atypica of Undetermined Significance or Follicular Lesion of Undetermined Significance) and (**c**) 6 Bethesda Category IV cytology (Follicular Neoplasm or Suspicious for a Follicular Neoplasm), with surgical histopathology. Benign nodules included both follicular adenomas and Hurthle cell adenomas. FNA: fine-needle aspiration.

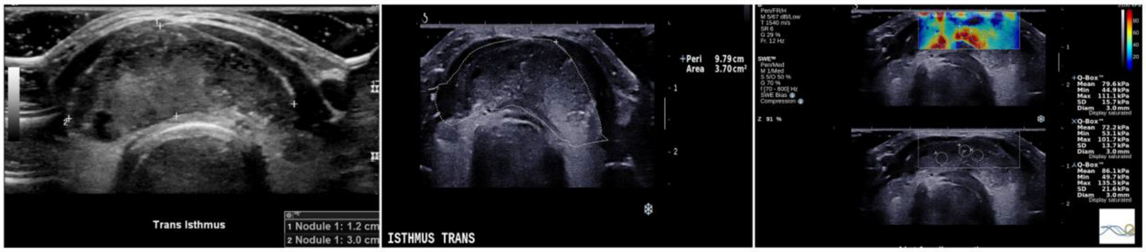

Figure 2: B-mode and shear wave elastography images.

The images are from a 36-year-old woman with papillary thyroid carcinoma. (**a**) Clinical B-mode image, (**b**) B-mode image obtained during the shear wave elastography study and (**c**) shear wave elastography map. The averaged minimum shear wave speed was 4.05 m/s. The greatest dimension was 30 mm. The corresponding f_{mass} value was 135 Hz.

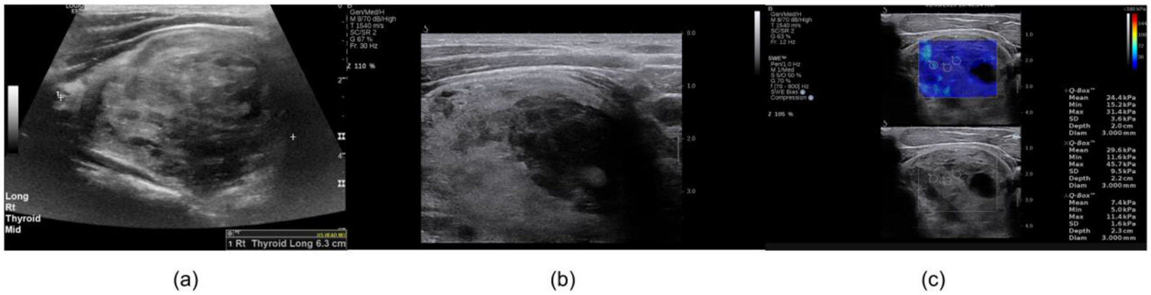

Figure 3: B-mode and shear wave elastography images.

The images are from a 41-year-old man with a Hurthle cell adenoma. (**a**) Clinical B-mode image, (**b**) B-mode image obtained during the shear wave elastography study and (**c**) shear wave elastography map. The averaged minimum shear wave speed was 1.88 m/s. The greatest dimension is 63 mm. The corresponding f_{mass} value was 29.8 Hz.

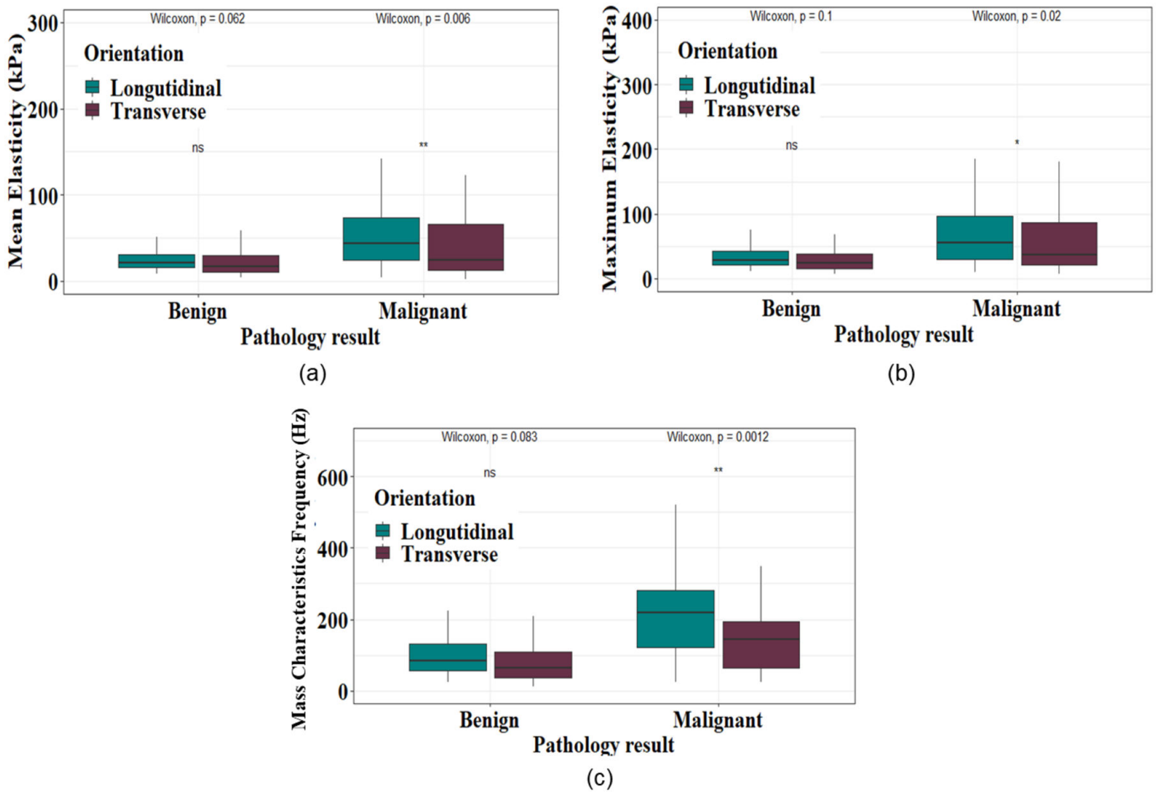

Figure 4: Comparison of shear wave elastography parameters between benign and malignant thyroid nodules.

(a) Comparison of the E_{mean} measured along the transverse and longitudinal orientations for benign and thyroid malignant nodules. **(b)** Comparison of the E_{max} measured along the transverse and longitudinal orientations for benign and malignant thyroid nodules. (**c**) Comparison of the f_{mass} measured along the transverse and longitudinal orientations for benign and malignant thyroid nodules. p value<0.05 indicates a statistical significance (* p<0.05, ** p<0.01).

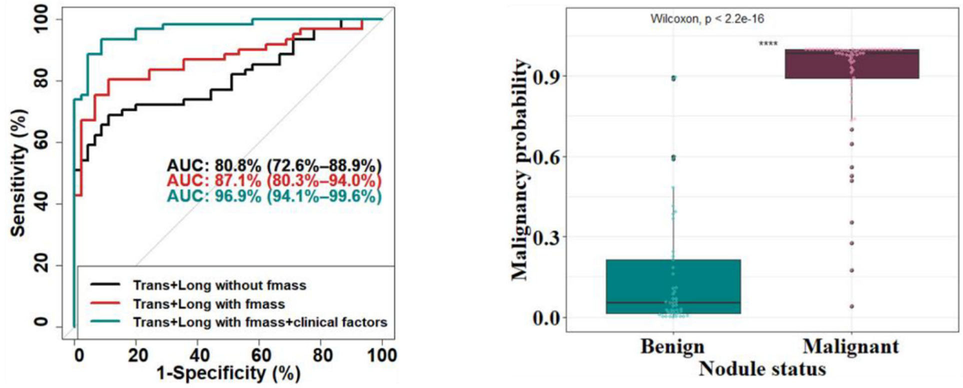

(a) (b)

Prediction model	AUC (95% CI)	Cutoff	Sensitivity	Specificity	PPV	NPV
Trans + Long without fmass (106)	80.8% (0.73-0.89)	0.601	68.9% (0.56-0.80)	88.9%(0.75-0.96)	89.4%(0.76-0.96)	67.8%(0.54-0.69)
Trans + Long with fmass (106)	87.1% (0.80-0.94)	0.520	80.3%()0.68-0.89	88.9%(0.75-0.96)	90.7%(0.79-0.97)	76.9%(0.63-0.87)
Trans + Long with fmass + clinical factors (106)	96.9% (0.94-1.00)	0.454	93.4%(0.83-0.98)	91.1%(0.79-0.97)	93.4%(0.83-0.98)	91.1%(0.78-0.97)

(c)

Figure 5: Ability of different prediction models to differentiate benign from malignant thyroid nodules.

(a) Receiver Operating Characteristic curves were generated using a multivariable logistic regression analysis to evaluate the ability of shear wave elasticity parameters with/without f_{mass} and with/without clinical factors to discriminate benign from malignant thyroid nodules. The black curve is "Trans + Long without f_{mass}", the red curve is "Trans + Long with f_{mass}", and the teal curve is "Trans + Long with f_{mass} + clinical factors". **(b)** The boxplot was calculated with the multivariable logistic regression analysis from the "Trans + Long with f_{mass} + clinical factors" model. **(c)** The summary of the ROC curves depicted in (a). Numbers in parentheses are the number of thyroid nodules included in the models. AUC: Area Under the Curve; Trans: Transverse; Long: Longitudinal; PPV: Positive Predictive Value; NPV: Negative Predictive Value.

Table 1:

Definition of shear wave parameters.

Elasticity parameter	Definition
E	shear wave elasticity
E_{mean_trans}	mean shear wave elasticity measured along the transverse orientation
E_{mean_long}	mean shear wave elasticity measured along the longitudinal orientation
E_{max_trans}	maximum shear wave elasticity measured along the transverse orientation
E_{max_long}	maximum shear wave elasticity measured along the longitudinal orientation
E_{sd}	standard deviation of the shear wave elasticity for each region of interest
E_{sd_trans}	E_{sd} measured along the transverse orientation
E_{sd_long}	E_{sd} measured along the longitudinal orientation
E_{mean_ratio}	$E_{mean\_long}/E_{mean\_trans}$
E_{sd_ratio}	E_{sd_long}/E_{sd_trans}
f_{mass}	$1000\ V_{min}/d$
f_{mass_trans}	f_{mass} along the transverse orientation
f_{mass_long}	f_{mass} along the longitudinal orientation

V_{min} is the minimum shear wave speed (m/s); d is the greatest dimension of the nodule measured from the B-mode images.

Table 2:

Summary of the parameters included in different prediction models

Model	SWE parameters	Clinical factors
Trans + Long without f_{mass}	E_{max_trans}, E_{sd_trans}, E_{mean_long}, E_{max_long}, E_{sd_long}, E_{mean_ratio}	
Trans + Long with f_{mass}	E_{mean_trans}, E_{sd_trans}, f_{mass_trans}, E_{max_long}, E_{sd_long}, E_{sd_ratio}, f_{mass_long}, f_{mass_trans}	
Trans + Long with f_{mass} + clinical factors	E_{sd_trans}, E_{mean_long}, E_{max_long}, E_{sd_long}, E_{sd_ratio}, f_{mass_trans}, f_{mass_long}	the presence of a cystic component, presence of punctate echogenic foci, nodule composition, gender

Table 3:

Comparison of shear wave elasticity parameters between benign and malignant thyroid nodules.

Elasticity Parameter	Benign	Malignant	p value*
E_{mean_trans} (kPa)	21.4 ± 14.7 (45)	44.0 ± 46.7 (62)	0.03
E_{max_trans} (kPa)	29.0 ± 17.9 (45)	63.4 ± 64.8 (62)	0.01
f_{mass_trans} (Hz)	82.7 ± 56.8 (45)	161.2 ± 124.8 (62)	<0.001
E_{mean_long} (kPa)	26.7 ± 17.6 (46)	63.9 ± 59.3 (66)	<0.001
E_{max_long} (kPa)	35.5 ± 22.4 (46)	82.1 ± 71.3 (66)	<0.001
f_{mass_long} (Hz)	103.0 ± 69.7 (46)	249.0 ± 189.3 (66)	<0.001

Note: Numbers are reported as mean ± standard deviation. Numbers in parentheses are the number of thyroid nodules. kPa: kilopascal; Hz: hertz.

*p value<0.05 indicates a statistical significance.

Table 4:

The effect of thyroid nodule macrocalcifications and peripheral rim calcifications on the elasticity parameter f_{mass_long}.

Parameter	Benign	p value*	Malignant	p value*
Macrocalcifications		0.96		0.02
Present (26)	92.6 + 45.8 (7)		331.8 + 239.7 (19)	
Absent (86)	104.9 + 73.4 (39)		215.5 + 155.5 (47)	
Peripheral Rim Calcifications		0.99		0.20
Present (9)	95.3 + 60.3 (4)		290.2 + 111.4 (5)	
Absent (103)	103.8 + 71.1 (42)		245.6 + 194.5 (61)	

Note: Numbers are mean ± standard deviation. Numbers in parentheses are the number of thyroid nodules.

*p value<0.05 indicates a statistical significance.